Supplement of Atmos. Chem. Phys., 22, 11409–11427, 2022
https://doi.org/10.5194/acp-22-11409-2022-supplement

Supplement of

Regional $PM_{2.5}$ pollution confined by atmospheric internal boundaries in the North China Plain: boundary layer structures and numerical simulation

Xipeng Jin et al.

Correspondence to: Xuhui Cai (xhcai@pku.edu.cn)

Text S1. Chemical transport model configuration

The air quality simulation was carried out to provide $PM_{2.5}$ concentration data and to conduct process analysis for wind shear category pollution. An advanced online-coupled meteorology-chemistry model, i.e., the Weather Research and Forecasting Model with Chemistry (WRF-Chem, version 4.1.1), was applied. The model domain, grid resolution, vertical levels, physical parameterization schemes, and simulation period were the same as the WRF model configurations in Sect. 2.2. The chemical initial and boundary conditions in the first run (three days earlier than the study period and the results were discarded as spin-up) were from the default data (an idealized profile for northern hemispheric, midlatitude, clean environment conditions) and then the outputs from the previous run were used as the initial and boundary conditions for the next run. The anthropogenic emissions of SO_2, NOx, CO, VOCs, NH_3, PM_{10}, $PM_{2.5}$, BC, OC, and CO_2 were set based on the MEIC database (Multi-resolution Emission Inventory for China; Li et al., 2017). Biogenic emissions were predicted online by WRF-Chem using the Model of Emissions of Gases and Aerosols from Nature (Guenther et al., 2006). We selected the Carbon Bond Mechanism version Z (CBMZ) mechanism to simulate gas-phase photochemical reactions (Zaveri and Peters, 1999) and the Model for Simulating Aerosol Interactions and Chemistry (MOSAIC) option with four discrete aerosol size bins to simulate aerosol interactions and chemistry (Zaveri et al., 2008). The modeled $PM_{2.5}$ concentrations were compared with the observations during Case-1 and Case-2, both from the time evolution and spatial distribution. The statistical results are presented in Table S2 and the simulated $PM_{2.5}$ concentration fields are shown in Fig. S4. The evaluation results demonstrate the reliability of the chemical transport model.

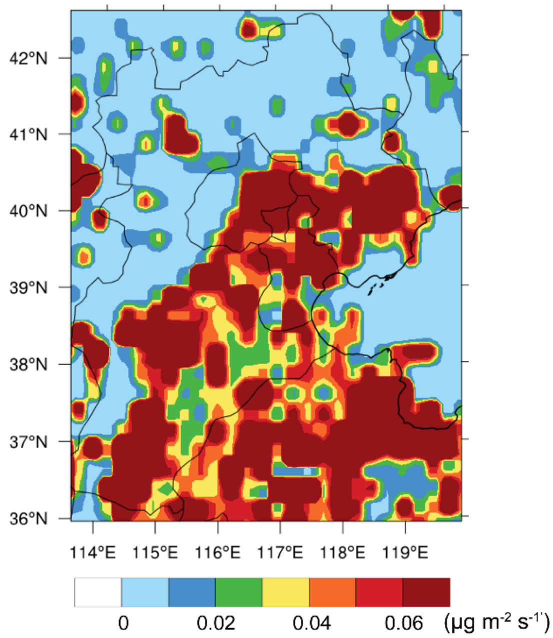

Figure S1. Spatial distribution of monthly mean $PM_{2.5}$ emission intensity in the North China Plain during wintertime of 2016 (The data comes from the website http://meicmodel.org).

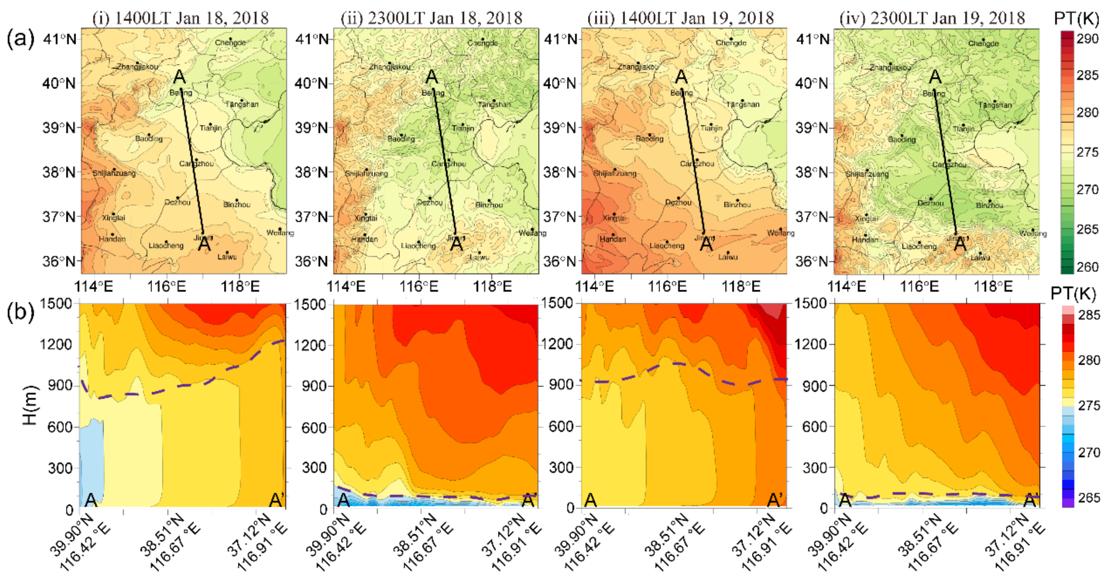

Figure S2. (a) Surface spatial distributions and (b) vertical cross-sections of the simulated potential temperature at the pollution stages of (i) formation, (ii-iv) maintenance, and (v) diffusion during representative Case-1 under west-southwest wind shear mode. The black lines in (a) indicate the section lines in (b). The purple dashed lines in (b) indicate the PBL heights.

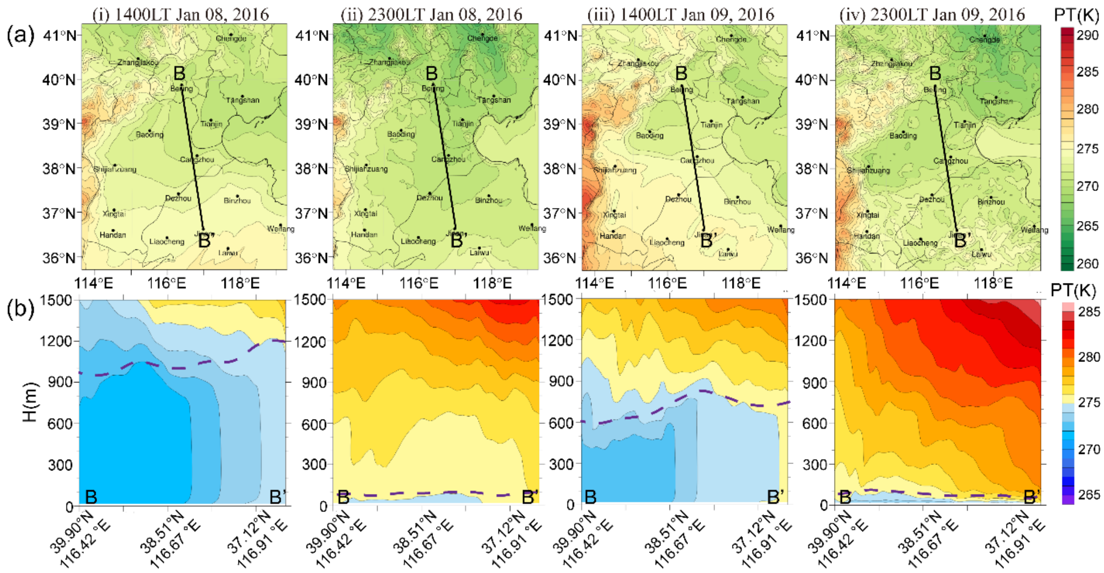

Figure S3. Same as Fig. S2, but for representative Case-2 under south-north wind shear mode.

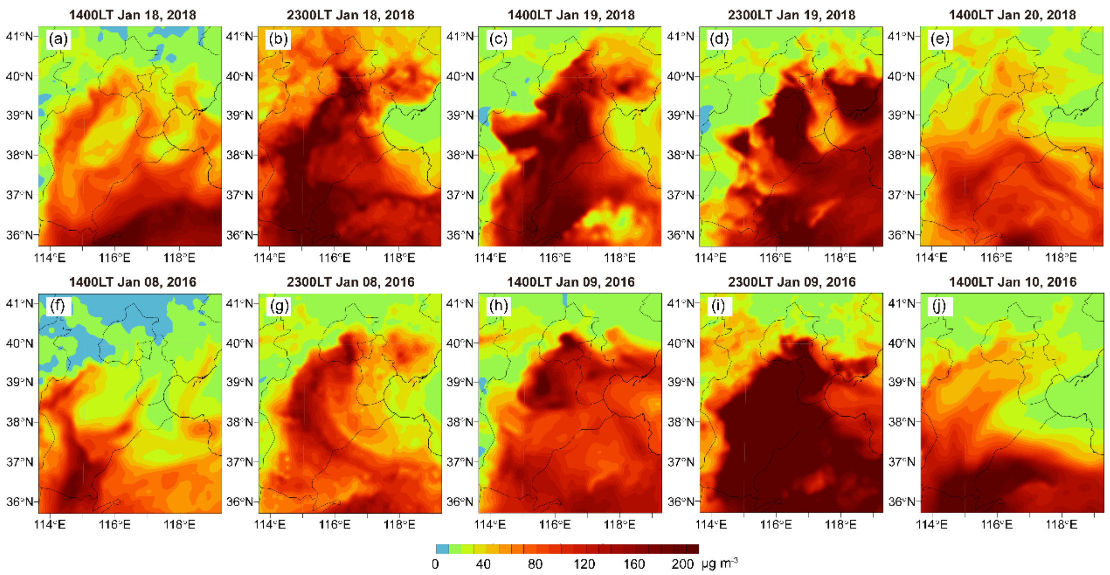

Figure S4. Simulated near-surface $PM_{2.5}$ concentrations during Case-1 (upper, representing west-southwest wind shear mode) and Case-2 (lower, representing south-north wind shear mode) at the pollution stages of (a, f) formation, (b-d, g-i) maintenance, and (e, j) diffusion.

Table S1. Statistics of model performance for the daily average near-surface potential temperature and 10 m wind speed for selected 13 cities during the representative cases.

	Case-1				Case-2				Case-3			
	PT (K)		**WS (m s^{-1})**		**PT (K)**		**WS (m s^{-1})**		**PT (K)**		**WS (m s^{-1})**	
	R	**RMSE**	**R**	**RMSE**	**R**	**RMSE**	**R**	**RMSE**	**R**	**RMSE**	**R**	**RMSE**
Beijing	0.99	0.94	0.91	0.65	0.89	2.99	0.72	1.67	0.74	1.84	0.94	1.20
Tianjin	0.99	1.14	0.99	1.03	0.96	2.46	0.67	1.48	0.90	1.71	0.62	1.90
Shijiazhuang	0.91	1.51	0.73	1.83	0.99	3.47	0.95	1.72	0.96	0.63	0.91	1.67
Baoding	0.79	0.73	0.84	0.82	0.98	2.55	0.99	1.03	0.93	1.34	0.83	1.59
Handan	0.98	1.00	1.00	0.19	0.90	2.33	0.96	1.14	0.99	0.69	0.78	1.64
Tangshan	0.86	1.61	0.94	0.77	1.00	3.14	0.98	0.53	0.71	2.45	0.89	2.00
Cangzhou	0.83	1.94	0.98	0.61	0.74	1.34	0.97	0.85	0.98	1.57	0.94	1.15
Dezhou	0.80	2.49	0.69	1.28	0.72	3.27	1.00	1.71	0.98	1.20	0.87	2.77
Jinan	0.79	1.61	0.80	1.46	0.99	3.71	0.99	1.57	0.94	1.17	0.66	2.38
Weifang	0.66	0.93	0.66	1.28	0.65	3.01	0.99	2.19	0.83	1.37	0.99	1.12
Binzhou	0.69	0.88	0.69	1.51	0.71	2.57	1.00	1.59	0.68	1.21	0.95	1.18
Chengde	0.72	3.66	0.76	1.55	0.70	5.14	0.97	0.80	0.81	2.87	0.96	1.29
Zhangjiakou	0.86	4.15	0.87	0.90	0.70	4.46	0.74	1.87	1.00	4.66	0.86	2.09
Average	**0.84**	**1.74**	**0.84**	**1.07**	**0.83**	**3.11**	**0.92**	**1.40**	**0.88**	**1.75**	**0.86**	**1.69**

Case-1: west-southwest wind shear mode (January 17–21, 2018); Case-2: south-north wind shear mode (January 7–11, 2016); Case-3: topographic obstruction category (October 7–12, 2014). R is the correlation coefficient and RMSE is the root mean square error.

Table S2. Statistics of model performance for the hourly near-surface $PM_{2.5}$ concentration for selected 13 cities during Case-1 and Case-2.

	Case-1		**Case-2**	
	R	**NMB**	**R**	**NMB**
Beijing	0.66	20%	0.61	18%
Tianjin	0.69	10%	0.69	9%
Shijiazhuang	0.57	-9%	0.75	-4%
Baoding	0.56	8%	0.88	10%
Handan	0.54	-11%	0.66	-14%
Tangshan	0.67	11%	0.59	25%
Cangzhou	0.63	-10%	0.63	-19%
Dezhou	0.52	3%	0.73	-25%
Jinan	0.54	-10%	0.71	-22%
Weifang	0.63	25%	0.79	12%
Binzhou	0.59	-12%	0.77	-2%
Chengde	0.62	4%	0.65	-30%
Zhangjiakou	0.67	8%	0.63	12%
Average	0.61	3%	0.70	-2%

Case-1: west-southwest wind shear mode (January 17–21, 2018); Case-2: south-north wind shear mode (January 7–11, 2016). R is the correlation coefficient and NMB is the normalized mean bias.

References

Guenther, A., Karl, T., Harley, P., Wiedinmyer, C., Palmer, P. I., and Geron, C.: Estimates of global terrestrial isoprene emissions using MEGAN (model of emissions of gases and aerosols from nature). Atmos. Chem. Phys., 6(11), 3181–3210. doi:10.5194/acp-6-3181-2006, 2006.

Li, M., Liu, H., Geng, G., Hong, C., Liu, F., Song, Y., Tong, D., Zheng, B., Cui, H. Y., Man, H. Y., Zhang, Q., and He, K. B.: Anthropogenic emission inventories in China: a review, Natl. Sci. Rev., 4, 834-866, doi: 10.1093/nsr/nwx150, 2017.

Zaveri, R. A., and Peters, L. K. (1999), A new lumped structure photochemical mechanism for large-scale applications. J. Geophys. Res.-Atmos., 104(D23), 30,387–30,415. doi:10.1029/1999JD900876, 1999.

Zaveri, R. A., Easter, R. C., Fast, J. D., and Peters, L. K.: Model for Simulating Aerosol Interactions and Chemistry (MOSAIC). J. Geophys. Res.-Atmos., 113, D13204. doi:10.1029/2007JD008782, 2008.